EUKARYOTIC CELL, Dec. 2007, p. 2278–2289 Vol. 6, No. 12
1535-9778/07/$08.00+0 doi:10.1128/EC.00349-07

Ssk2 Mitogen-Activated Protein Kinase Kinase Kinase Governs Divergent Patterns of the Stress-Activated Hog1 Signaling Pathway in *Cryptococcus neoformans*▽†

Yong-Sun Bahn,[1] Scarlett Geunes-Boyer,[2] and Joseph Heitman[3]*

Department of Bioinformatics and Life Science, Soongsil University, Seoul, Korea,[1] and Departments of Cell Biology,[2] Molecular Genetics and Microbiology, Medicine, and Pharmacology and Cancer Biology,[3] Duke University Medical Center, Durham, North Carolina 27710

Received 24 September 2007/Accepted 8 October 2007

The stress-activated p38/Hog1 mitogen-activated protein kinase (MAPK) pathway is structurally conserved in many diverse organisms, including fungi and mammals, and modulates myriad cellular functions. The Hog1 pathway is uniquely specialized to control differentiation and virulence factors in a majority of clinical *Cryptococcus neoformans* serotype A and D strains. Here, we identified and characterized the Ssk2 MAPKKK that functions upstream of the MAPKK Pbs2 and the MAPK Hog1 in *C. neoformans*. The *SSK2* gene was identified as a potential component responsible for the difference in Hog1 phosphorylation between the serotype D f1 sibling strains B-3501 and B-3502 through comparative analysis of meiotic maps showing their meiotic segregation patterns of Hog1-dependent sensitivity to the antifungal drug fludioxonil. Ssk2 is the only component of the Hog1 MAPK cascade that is polymorphic between the two strains, and the B-3501 and B-3502 *SSK2* alleles were distinguished by two coding sequence changes. Supporting this finding, *SSK2* allele exchange completely interchanged the Hog1-controlled signaling patterns, related phenotypes, and virulence levels of strains B-3501 and JEC21. In the serotype A strain H99, disruption of the *SSK2* gene enhanced capsule and melanin biosynthesis and mating efficiency, similar to *pbs2* and *hog1* mutations. Furthermore, *ssk2*Δ, *pbs2*Δ, and *hog1*Δ mutants were hypersensitive to a variety of stresses and resistant to fludioxonil. In agreement with these results, Hog1 phosphorylation was abolished in the *ssk2*Δ mutant, similar to what occurred in the *pbs2*Δ mutant. Taken together, these findings indicate that Ssk2 is a critical interface connecting the two-component system and the Pbs2-Hog1 MAPK pathway in *C. neoformans*.

All living organisms constantly encounter environmental stresses and must give responses to maintain cellular homeostasis and survive. Sensing stress is particularly critical for pathogenic microorganisms that must overcome the hostile host environment during infection. To sense, transduce, and respond to a plethora of external stimuli, cells employ stress-activated mitogen-activated protein kinase (MAPK) signaling pathways.

In mammals, two MAPKs, p38 and Jun N-terminal kinase, mediate stress-activated signaling pathways (for reviews, see references 20 and 25). The murine p38 MAPK was first identified as a kinase activated in response to bacterial lipopolysaccharide (LPS). Humans have four p38 MAPK family members, α, β, γ, and δ, among which p38 α and p38 β are ubiquitously expressed in most tissues. The major role of p38 MAPKs includes transduction of stress-related signals, including osmotic shock and radiation, apoptosis, and regulation of an immune response, such as cytokine production and inflammation. Members of the p38 MAPK family are activated by upstream MAPK kinases (MAPKKs), including MKK6 and MKK3, which dually phosphorylate Thr and Tyr residues in a Thr-Gly-Tyr (TGY) motif. These MAPKKs are activated by phosphorylation on Ser and Thr by MEKK4 (MAP or extracellular signal-regulated kinase kinase kinase), ASK1 (apoptosis-stimulated kinase), or TAK1 (transforming growth factor β-activated kinase).

The stress-activated MAPK pathway is evolutionarily conserved in fungi. The closest fungal ortholog of p38 MAPK is Hog1, which was first identified via its role in modulating responses to osmotic shock in the model yeast *Saccharomyces cerevisiae* (8, 18). Similar to mammalian p38, Hog1 contains the TGY motif in which Thr and Tyr residues are dually phosphorylated by the MAPKK Pbs2 (8). Pbs2 is activated by three MAPKK kinases (MAPKKKs), including Ssk2, Ssk22, and Ste11 (26, 32). Hog1 orthologs have been identified and characterized for other fungi, including Sty1/Spc1 in *Schizosaccharomyces pombe* (28), Hog1 in *Candida albicans* (1), SakA in *Aspergillus nidulans* (21), and Osm1 in *Magnaporthe grisea* (7). Interestingly, the fungal Hog1 MAPK not only modulates a variety of stress responses but also governs many central cellular processes, such as sexual development and morphological differentiation.

Upstream signaling pathways for the p38/Hog1 MAPKs are strikingly different in fungi and mammals. In humans, the p38 MAPK module is activated by a wealth of upstream signaling components, including GADD45-like proteins, G-protein-coupled receptors associating with Rac/Cdc42 and p20-activated kinase, and tyrosine kinases (25). In contrast, fungal Hog1 MAPK modules are mainly controlled by two-component

* Corresponding author. Mailing address: Department of Molecular Genetics and Microbiology, 322 CARL Building, Box 3546, Research Drive, Duke University Medical Center, Durham, NC 27710. Phone: (919) 684-2824. Fax: (919) 684-5458. E-mail: heitm001@duke.edu.

† Supplemental material for this article may be found at http://ec.asm.org/.

▽ Published ahead of print on 19 October 2007.

phosphorelay systems (7, 18). In *S. cerevisiae*, although the Hog1 MAPK can be also activated by the Sho1 and Msb2 transmembrane proteins, the two-component system, which comprises the hybrid histidine kinase (HK) Sln1, the histidine-containing phosphotransfer protein Ypd1, and the response regulator Ssk1, mainly controls the Ssk2/Ssk22-Pbs2-Hog1 MAPK pathway (18). Similar to the model yeast, other fungi employ the two-component system as a major upstream controller for the Hog1 MAPK pathway (7, 9).

We previously identified and characterized the stress-activated Hog1 MAPK in the basidiomycetous fungus *Cryptococcus neoformans* (5). This human fungal pathogen normally inhabits natural environments, such as trees, soil, and pigeon guano, and following its inhalation into the alveoli of the lung, it disseminates to cause severe fungal meningitis, mostly in immunocompromised patients (19). The *C. neoformans* Pbs2-Hog1 MAPK pathway not only modulates responses to a plethora of stresses, including osmotic shock, UV, high temperature, and oxidative stress, but also controls sexual development by repressing pheromone production (5). Unexpectedly, two major virulence factors of *C. neoformans*, the polysaccharide antiphagocytic capsule and the antioxidant melanin, are negatively regulated by Hog1, possibly via cross talk with the cyclic AMP (cAMP)-protein kinase A signaling pathway and other signaling pathways (5). More recently, we also identified and characterized a two-component-like system upstream of the Pbs2-Hog1 signaling pathway (6). The *C. neoformans* two-component system consists of two response regulators, Ssk1 and Skn7; the histidine-containing phosphotransfer protein Ypd1; and seven hybrid HKs (Tco1 to Tco7). Among the seven HKs, two, Tco1 and Tco2, play redundant roles in controlling the Pbs2-Hog1 MAPK pathway (6).

A defining difference between the *C. neoformans* Hog1 MAPK and those of other fungi is the regulation of the former by phosphorylation. Strikingly, the Hog1 MAPK is constitutively phosphorylated under normal conditions and dephosphorylated upon stress, such as osmotic shock, in a majority of *C. neoformans* strains, including the serotype A H99 and serotype D B-3501 strains, which are the platform strains for the genome sequencing project (5). In contrast, in some *C. neoformans* strains, including the serotype D strain JEC21 and its f1 sibling strain B-3502 (equivalent to JEC20), Hog1 is not phosphorylated under normal conditions but is rapidly phosphorylated upon stress, similar to what occurs in *S. cerevisiae* and other fungi (5). The constitutive phosphorylation of the Hog1 MAPK appears to confer unique phenotypic characteristics to *C. neoformans*. First, strains containing constitutively phosphorylated Hog1 are generally more stress resistant than strains having nonphosphorylated Hog1. Second, hypermating ability induced via derepressed pheromone production and hyperproduction of capsule and melanin are observed in strains expressing constitutively phosphorylated Hog1. Finally, constitutive Hog1 phosphorylation results in marked sensitivity to the antifungal drug fludioxonil, which activates Hog1 signaling to increase intracellular glycerol content, causes cell swelling and cytokinesis defects, and ultimately inhibits cell growth (22).

Genetics strives to define the functions of wild-type (WT) gene products via analysis of mutant alleles, often isolated following genome-wide mutagenic screens, or targeted gene disruption following transformation and homologous recombination. While these remain powerful genetic tools, an alternative approach seeks to define the genetic diversity that occurs naturally in a given population. The recent advent of genomics has considerably advanced this approach, enabling rigorous genome-wide mapping and population genetics analysis. Here, we have applied such an approach for the human fungal pathogen *C. neoformans* to analyze differences in phenotypic characteristics in two strains that have been subject to complete genome analysis (JEC21 and B-3501). Genetic crosses, high-resolution meiotic mapping, and comparative genomics were marshaled to define a Mendelian trait that confers resistance or sensitivity to multiple cell stress responses, typified by the action of the drug fludioxonil, which activates the Hog1 osmostress cascade. A 250-kb region linked to the phenotype of interest was defined, and among the 86 candidate genes in this interval, the *SSK2* gene encoding an upstream MAPKKK element of the Hog1 pathway was shown to be responsible for the variation naturally occurring in the population, based on linkage analysis and allele exchange experiments. These studies highlight the application of genome-wide meiotic mapping and comparative genomics to define virulence attributes of pathogenic microorganisms.

MATERIALS AND METHODS

Strains and media. The strains used in this study are listed in Table 1. B-3501 (*MAT*α) and B-3502 (*MAT***a**; equivalent to JEC20) are derived from the parental strains of NIH12 (a clinical isolate) and NIH433 (an environmental isolate) (16). Yeast extract-peptone-dextrose (YPD), V8 medium for mating, Niger seed medium for melanin production, and agar-based Dulbecco's modified Eagle's medium (DMEM) for capsule production were all as previously described (2, 4, 14, 17).

Identification of the *SSK2* MAPKKK gene by comparative meiotic mapping. To identify the genomic locus responsible for the differences in constitutive Hog1 phosphorylation levels between B-3501 and B-3502 (equivalent to JEC20), fludioxonil resistance/sensitivity, which is directly related to Hog1 phosphorylation patterns (22), was measured in 94 f1 progeny from a cross between strains B-3501 and B-3502. The 94 progeny were incubated overnight at 30°C in 96-well plates containing YPD medium, serially diluted (1 to 10^4 dilutions) in distilled water (dH_2O), and spotted (3 μl) onto solid YPD medium containing 100 μg/ml of fludioxonil (100 mg/ml stock solution in dimethyl sulfoxide; Sigma-Aldrich, St. Louis, MO). Plates were incubated for 2 to 3 days and photographed. Data were analyzed using JoinMap 3.0 software. To verify whether the *SSK2* allele difference is directly related to fludioxonil resistance or sensitivity, diagnostic PCR was performed with primers specific for the B-3501 *SSK2* allele (14739/14699) and the B-3502 *SSK2* allele (14696/14697) and genomic DNAs of the 94 progeny from B-3501 and B-3502, which were kindly provided by Tom Mitchell's laboratory (Duke University).

Disruption of the *SSK2* gene and complementation of the *ssk2*Δ mutant. To investigate the role of Ssk2, the *SSK2* gene was disrupted in the serotype D strains JEC21 and B-3501 and the serotype A strain H99 by overlap PCR followed by biolistic transformation as previously described (5, 11). Primers for amplification of the 5′ and 3′ flanking regions of the *SSK2* gene in H99, JEC21, and B-3501 strains are listed in Table S1 in the supplemental material. M13 reverse and forward primers were used to amplify the dominant selectable markers, Nat^r and Neo^r. Each gel-extracted gene disruption cassette was precipitated onto 600 μg of gold microcarrier beads (0.8 μm; Bioworld Inc., Dublin, OH), and the indicated serotype A and D strains were biolistically transformed as described previously (12). Stable transformants were selected on YPD medium containing nourseothricin or G418. Each mutant strain was first screened by diagnostic PCR and further confirmed by Southern blot analysis (not shown) using gene-specific probes prepared with primers listed in Table S1 in the supplemental material.

To authenticate *ssk2*Δ mutant phenotypes, *ssk2*Δ+*SSK2* complemented strains were constructed as follows. First, genomic DNA containing the full-length *SSK2* gene was screened using *SSK2* gene-specific probes (see Table S1 in the supplemental material) from *C. neoformans* H99, JEC21, and B-3501 bacterial artificial chromosome (BAC) libraries. With the BAC clones as a template,

TABLE 1. Strains used in this study[a]

Serotype and strain	Genotype (serotype)	Parent	Source or reference
A			
H99	*MAT*α		30
KN99**a**	*MAT***a**		29
YSB330	*MAT*α *mkk1*Δ::*NAT-STM#224*	H99	22
KK3	*MAT*α *mpk1*Δ::*NAT-STM#150*	H99	22
YSB64	*MAT*α *hog1*Δ::*NAT-STM#177*	H99	5
YSB81	*MAT***a** *hog1*Δ::*NEO*	KN99	5
YSB123	*MAT*α *pbs2*Δ::*NAT-STM#213*	H99	5
YSB125	*MAT***a** *pbs2*Δ::*NEO*	KN99	5
YSB261	*MAT*α *ssk1*Δ::*NAT-STM#205*	H99	6
YSB429	*MAT***a** *ssk1*Δ::*NAT-STM#205*	KN99	6
YSB349	*MAT*α *skn7*Δ::*NAT-STM#201*	H99	6
YSB313	*MAT*α *ste11*Δ::*NAT-STM#242*	H99	This study
YSB342	*MAT*α *ste7*Δ::*NAT-STM#225*	H99	This study
YSB345	*MAT***a** *ste7*Δ::*NEO*	KN99	This study
YSB127	*MAT*α *cpk1*Δ::*NAT-STM#184*	H99	This study
YSB130	*MAT***a** *cpk1*Δ::*NEO*	KN99	This study
YSB273	*MAT*α *bck1*Δ::*NAT-STM#43*	H99	22
YSB264	*MAT*α *ssk2*Δ::*NAT-STM#210*	H99	This study
YSB441	*MAT***a** *ssk2*Δ::*NAT-STM#210*	KN99	This study
YSB367	*MAT*α *ssk2*Δ::*NAT-STM#210 SSK2-NEO*	YSB264	This study
D			
JEC21	*MAT*α		24
JEC20 (B-3502)	*MAT***a**		24
B-3501	*MAT*α		24
YSB267	*MAT*α *pbs2*Δ::*NAT-STM#213*	JEC21	This study
YSB139	*MAT*α *hog1*Δ::*NAT-STM#177*	JEC21	5
YSB143	*MAT***a** *hog1*Δ::*NEO*	JEC20	5
YSB338	*MAT*α *ssk2*Δ::*NAT-STM#210*	JEC21	This study
YSB368	*MAT*α *ssk2*Δ::*NAT-STM#210 SSK2-NEO*	YSB338	This study
YSB340	*MAT*α *ssk2*Δ::*NAT-STM#210*	B-3501	This study
YSB391	*MAT*α *ssk2*Δ::*NAT-STM#210 SSK2-NEO*	YSB340	This study
YSB392	*MAT*α *ssk2*Δ::*NAT-STM#210 SSK2*(B-3501)*-NEO*	YSB338	This study
YSB394	*MAT*α *ssk2*Δ::*NAT-STM#210 SSK2*(B-3501)*-NEO*	YSB338	This study

[a] Each *NAT-STM#* indicates the Nat^r marker with a unique signature tag.

DNA fragments containing the complete *SSK1* gene (5.8 kb in strain H99 [*SSK2-A*], 5.7 kb in strain JEC21 [*SSK2-J*], and 5.6 kb in strain B-3501 [*SSK2-B*]) were PCR amplified with primers 15332/15333 (H99 BAC clones) and 15334/15335 (JEC21 and B-3501 BAC clones) and cloned into the pCR2.1-TOPO vector (Invitrogen, Carlsbad, CA). Each insert was confirmed by DNA sequencing and subcloned into plasmid pJAF12 (Neo^r), generating plasmids pNEOSSK2A, pNEOSSK2J, and pNEOSSK2B to complement the *ssk2-A*Δ (strain H99 background), *ssk2-J*Δ (strain JEC21 background), and *ssk2-B*Δ (strain B-3501 background) mutants, respectively. For the targeted reintegration of the *SSK2* allele into its native locus in the H99 strain (*ssk2-A*Δ+*SSK2-A*), pNEOSSK2A was linearized by PflMI digestion and strain *ssk2-A*Δ (YSB264) was biolistically transformed (Table 1). For the targeted reintegration of the *SSK2* allele into its native locus in the JEC21 (*ssk2-J*Δ+*SSK2-J*) and B-3501 (*ssk2-B*Δ+*SSK2-B*) strains, plasmids pNEOSSK2J and pNEOSSK2B were linearized by MfeI digestion, and *ssk2-J*Δ (YSB338) and *ssk2-B*Δ (YSB340), respectively, were biolistically transformed.

***SSK2* allele exchange between JEC21 and B-3501.** To exchange the *SSK2* allele between strains JEC21 and B-3501, the *ssk2-J*Δ (YSB338) mutant was biolistically transformed with MfeI-digested, linearized pNEOSSK2B targeting to the native *SSK2-J* locus. Stable *SSK2* allele-exchanged transformants were selected on YPD medium containing G418. *SSK2* allele-exchanged strains (*ssk2-J*Δ+*SSK2-B*; YSB392 and YSB394) were confirmed by Southern blot analysis (data not shown). To further confirm the target-specific exchange of the *SSK2* alleles, the *SSK2* allele and its upstream and downstream genetic markers, MspI and Eco20, respectively, were PCR amplified by primers listed in Table S1 in the supplemental material and analyzed with 1% agarose gel. PCR products for the MspI and Eco20 markers were further digested by MspI and EcoRI and analyzed with a 1% agarose gel.

Assay for capsule and melanin production and mating. Capsule and melanin production were monitored using agar-based DMEM and Niger seed medium, respectively, as described previously (4, 17). The capability for mating between α and **a** cells was measured with V8 medium (pH 5.0), and the relative pheromone production levels were monitored by confrontation assays as previously described (4, 17). Images of mating and confrontation assays were captured with a Nikon Eclipse E400 microscope equipped with a Nikon DXM1200F digital camera.

Sensitivity test for stress responses, fludioxonil, and methylglyoxal. Each strain was incubated overnight at 30°C in YPD medium, washed with sterile dH_2O, serially diluted (1 to 10^4 dilutions) in dH_2O, and spotted (3 μl) onto solid YPD medium containing the indicated concentrations of NaCl or KCl for osmotic shock or onto solid YPD medium containing the indicated concentrations of H_2O_2 for oxidative stress. To test sensitivity to UV irradiation, cells spotted on solid YPD medium were exposed to UV for 0.2 (480 J/m^2) or 0.3 (720 J/m^2) min, using a UV Stratalinker (model 2400; Stratagene). To test temperature sensitivity, plates were incubated at 30 and 40°C. For tests of sensitivity to fludioxonil, cells were spotted on solid YPD medium containing the indicated concentrations of fludioxonil (Sigma-Aldrich) or methylglyoxal (Sigma-Aldrich). Each plate was incubated for 2 to 3 days and photographed.

Western blot analysis of Hog1 phosphorylation. Yeast cells were grown to mid-logarithmic phase as described above, and an equal volume of YPD medium containing 2 M NaCl (final 1 M NaCl) or the indicated concentrations of fludioxonil or methylglyoxal were added. A fraction of the culture at each time point was rapidly frozen in a dry ice-ethanol bath, resuspended in lysis buffer (5) with 1.0 to 1.2 g of acid-washed glass beads (425 to 600 μm; Sigma-Aldrich), and disrupted using a bead beater. Protein concentrations for each sample were measured with the Bio-Rad protein assay reagent, and equal amounts of protein were loaded into a 10% Tris-glycine gel (Novex, San Diego, CA). Separated proteins were transferred to an immunoblot polyvinylidene difluoride membrane (Bio-Rad, Hercules, CA) and incubated overnight at 4°C, with a rabbit p38-MAPK-specific antibody (Cell Signaling Technology, Beverly, MA) as the primary antibody and a horseradish peroxidase-conjugated anti-rabbit immuno-

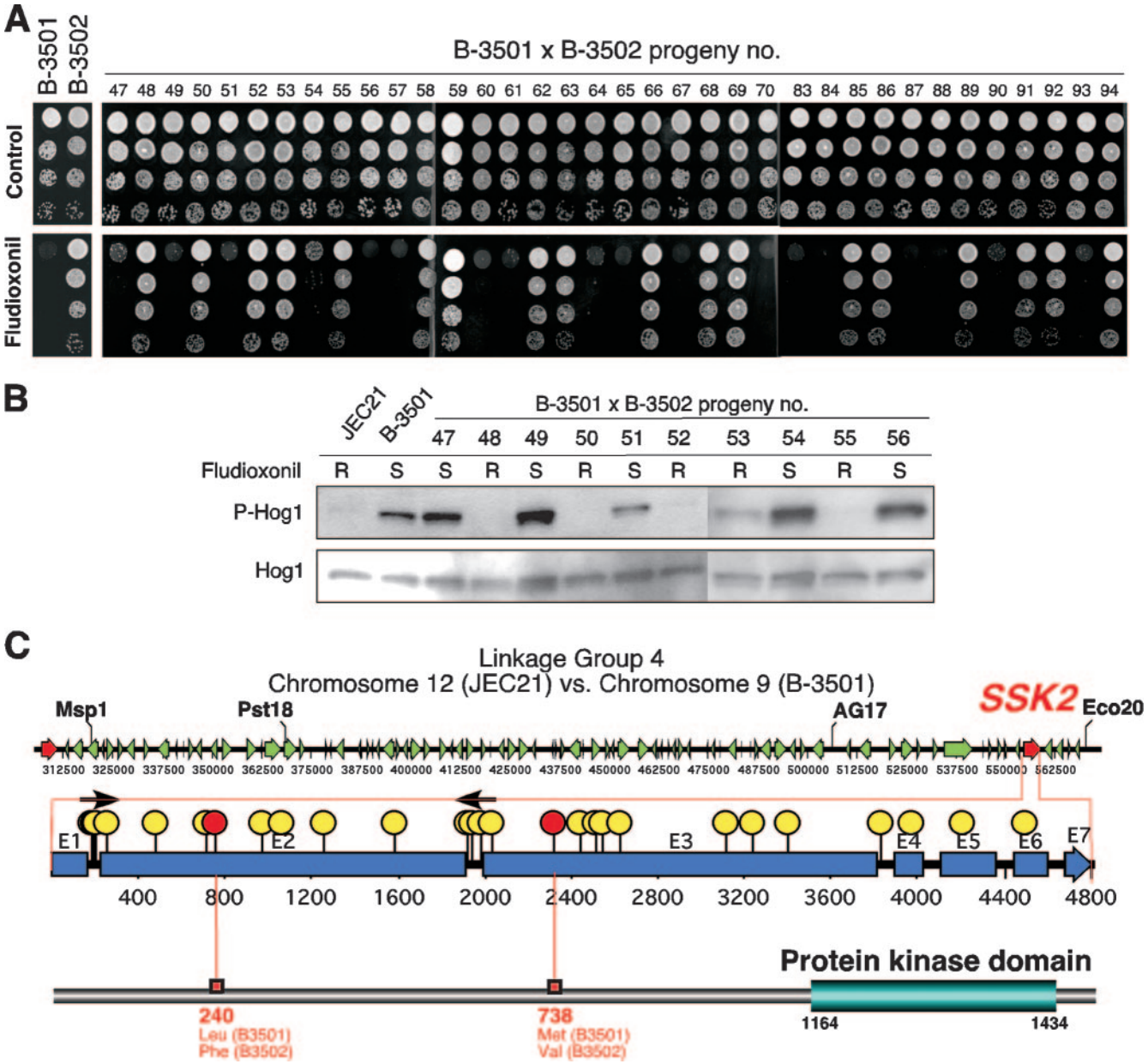

FIG. 1. Identification of the genomic locus responsible for differential Hog1-dependent fludioxonil sensitivity in *C. neoformans* by meiotic mapping. (A) Ninety-four f1 progeny from the B-3501 and B-3502 mating were grown overnight at 30°C in YPD medium, and 3 μl of culture was spotted on solid YPD medium with or without fludioxonil (10 μg/ml). The plates were further incubated at 30°C for 2 days and photographed. Among the 94 progeny, results for fludioxonil sensitivity/resistance of 36 progeny (no. 47 to 70 and no. 83 to 94) are shown here. (B) WT *C. neoformans* serotype D strains (JEC21 and B-3501) and 10 progeny from the B-3501 and B-3502 mating (no. 47 to 56) were grown to mid-logarithmic phase, and total protein extracts were prepared for Western blot analysis. The dual phosphorylation status of Hog1 (T171 and Y173) was monitored using anti-dually phosphorylated p38 antibody (P-Hog1). The same blots were stripped and then probed with polyclonal anti-Hog1 antibody as a loading control (Hog1). R, resistant; S, sensitive. (C) Chromosomal region between MspI and Eco20 markers (linkage group 4 of chromosome 12 in JEC21 or chromosome 9 in B-3501) is illustrated, with arrows indicating the annotated ORFs. Among the 86 ORFs in the region, the genomic DNA sequences for the *SSK2* genes from JEC21 and B-3501 were compared. Yellow and red circles indicate synonymous and nonsynonymous changes, respectively.

globulin G antibody as the secondary antibody, for detection of phosphorylated Hog1. The blot was developed using an enhanced chemiluminescence Western blotting detection system (GE Healthcare, Little Chalfont, Buckinghamshire, United Kingdom). Subsequently, the blot was stripped and further used for detection of Hog1, with a rabbit polyclonal anti-Hog1 antibody (Santa Cruz Biotechnology, Santa Cruz, CA) as a loading control.

Macrophage assays. The MH-S murine alveolar macrophage cell line (ATCC, Manassas, VA) was maintained in RPMI 1640 containing 10% HyClone heat-inactivated fetal bovine serum, 2 mM L-glutamine, 1 mM sodium pyruvate, 4.5 g/l glucose, 1.5 g/l bicarbonate, 0.05 mM 2-mercaptoethanol, and penicillin-streptomycin at 37°C with 5% CO_2. Macrophages were harvested from monolayers with TrypLE Express (Invitrogen, Carlsbad, CA), and cell viability was deter-

TABLE 2. Fludioxonil sensitivity segregation patterns in B-3501 and B-3502 progeny

Marker name	No. of progeny with indicated pattern	
	Uncoupled	Coupled
Hae5	23	71
Eco20	9	85
AG17	3	91
Pst18	2	92
MspI	19	75

mined by trypan blue exclusion and cell counts. Macrophages were adjusted to a concentration of 10^6/ml, and 100 μl of this suspension was added to flat-bottom 96-well plates (Corning Incorporated, Corning, NY) and allowed to adhere. Macrophages were stimulated with 200 units/ml recombinant gamma interferon murine (Cell Sciences, Canton, MA) and 100 ng/ml LPS (0111:B4) for 3 h. One hundred microliters of complete medium was added, and cells were incubated overnight prior to yeast challenge. Fungal cells were washed three times in sterile phosphate-buffered saline, counted with a hemocytometer, adjusted to a concentration of 10^7 cell/ml in culture medium, and added (10^5 cells in 10 μl) to the MH-S cells at a multiplicity of infection of 1:1. Control wells contained only yeasts or macrophages. Immunoglobulin G1 anti-GXM monoclonal antibody was added to yeast inocula as opsonin at a final concentration of 2 μg/ml. Macrophage-yeast mixtures were incubated for 12 h, and quantitative cultures were performed by aspirating the medium from each well and lysing the remaining macrophages with two exchanges of 100 μl of 0.01% sodium dodecyl sulfate. The aspirated medium and sodium dodecyl sulfate solutions were combined and cultured on YPD agar medium for 2 to 3 days at 30°C. Multiple dilutions were examined, and at least 100 colonies were counted for each plate. All experiments compared the results for five replicate wells of each strain with similar results obtained for two independent experiments. The quantitative culture data were combined, and statistical analyses were performed using one-way analysis of variance (Bonferroni's multiple comparison test). Results are expressed as percents decrease in CFU relative to yeast-only (no macrophage) control levels.

RESULTS AND DISCUSSION

Ssk2 MAPKKK mediates unique regulation patterns of the Hog1 MAPK. To identify the key signaling component contributing to the divergent phosphorylation patterns of Hog1 MAPK observed in different clinical and environmental *C. neoformans* isolates, we took advantage of the fact that Hog1 is constitutively phosphorylated in strain B-3501 but not in B-3502 (5). Based on a prior report analyzing a meiotic map of 94 progeny derived from mating between strains B-3501 and B-3502 (27), we monitored the fludioxonil sensitivity/resistance of the 94 progeny, a phenotype directly correlated with constitutive phosphorylation of Hog1 (23). Previously, we have shown that fludioxonil treatment hyperactivates Hog1, which elicits overaccumulation of intracellular glycerol and causes cell swelling and eventually growth inhibition (23). Therefore, strain B-3501, in which Hog1 is constitutively phosphorylated, is highly sensitive to fludioxonil whereas strain B-3502, in which Hog1 is not constitutively phosphorylated, is resistant (23). Among the 94 progeny tested, 44 exhibited fludioxonil resistance and 50 fludioxonil sensitivity, which is a typical 1:1 Mendelian segregation pattern (Fig. 1A), indicating that the difference in fludioxonil sensitivity between strains B-3501 and B-3502 is an inheritable genetic trait attributable to a single gene. We also monitored other Hog1-related phenotypes, including high-temperature resistance, hydrogen peroxide sensitivity, and osmotic shock resistance, in the 94 progeny, and all of these phenotypes were found to be quantitative polygenic traits (data not shown). Particularly for hydrogen peroxide sensitivity, however, the segregation patterns among the 94 progeny were closely correlated with fludioxonil sensitivity (data not shown).

To confirm whether fludioxonil sensitivity is correlated with constitutive Hog1 phosphorylation, we monitored the Hog1 phosphorylation levels of 10 progeny (no. 47 to 56) under unstressed conditions by Western blot analysis. Similar to what was found for strain B-3501, the f1 progeny exhibiting fludioxonil sensitivity showed higher levels of Hog1 phosphorylation than the fludioxonil-resistant progeny (Fig. 1B).

Subsequently, we compared the fludioxonil sensitivity data with the previously reported meiotic map of the 94 progeny (27). As summarized in Table 2 and Table S2 in the supplemental material, fludioxonil sensitivity was closely correlated with the Pst18 (97.9% coupling) and AG17 (96.8% coupling) markers in linkage group 4 of chromosome 12 of JEC21 or chromosome 9 of B-3501. Other markers flanking Pst18 and AG17 are Eco20 and MspI (Fig. 1B), and fludioxonil sensitivity was more closely linked to the Eco20 (90.4% coupling) than to the MspI (79.8% coupling) marker (Table 2). Therefore, a gene encoding a potential signaling component was predicted to be located between the Pst18/AG17 and Eco20 genetic markers (Fig. 1C). In the 250-kb region (between MspI and Eco20) of JEC21 chromosome 12, all of the annotated open reading frames (ORFs) were analyzed and a potential Hog1 signaling component that is highly homologous to the *S. cerevisiae* Ssk2 MAPKKK was found (Fig. 1C). In fact, the *SSK2* gene is located between the AG17 and Eco20 markers, as would be predicted for relevant candidate genes, based on the fludioxonil segregation data.

S. cerevisiae Ssk2 is known to phosphorylate and activate the MAPKK Pbs2 (31). The B-3501 and B-3502 *SSK2* alleles are polymorphic, including two coding sequence changes (Fig. 1C). To further support this finding, the *SSK2* alleles were typed in all 94 f1 progeny by using *SSK2* allele-specific primers. The *SSK2* allele segregation patterns were completely linked to the

FIG. 2. *SSK2* allele segregation in B-3501/B-3502 meiotic progeny. Allele-specific PCR was performed with *SSK2* allele specific primers (14696/14697 for B-3501 *SSK2* and 14699/14739 for B-3502 [or JEC21]) and genomic DNA of the 94 progeny from B-3501 and B-3502 mating and analyzed with a 1% agarose gel. Similar to what appears in Fig. 1A, among the 94 progeny, results for allele-specific PCRs of 36 progeny (no. 47 to 70 and no. 83 to 94) are shown here. Fludio., fludioxonil; R, resistant; S, sensitive.

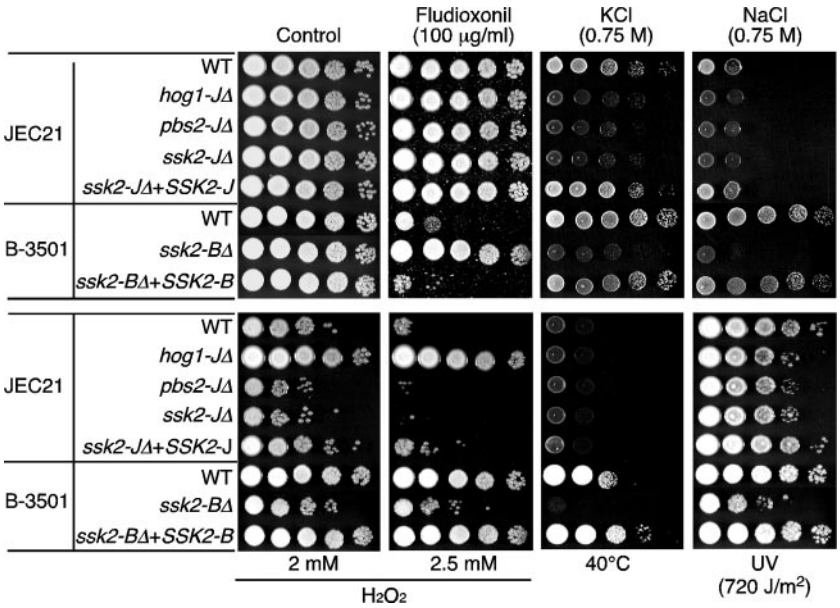

FIG. 3. Ssk2 MAPKKK modulates *C. neoformans* stress responses. Each *C. neoformans* strain (for the serotype D JEC21 lineage, WT JEC21, YSB139 [*hog1-J*Δ], YSB267 [*pbs2-J*Δ], YSB338 [*ssk2-J*Δ], and *ssk2-J*Δ+*SSK2-J*-complemented YSB368; for the serotype D B-3501 lineage, WT B-3501, YSB340 [*ssk2-B*Δ], and *ssk2-B*Δ+*SSK2-B*-complemented YSB391) was grown to mid-logarithmic phase in YPD medium and 10-fold serially diluted (1 to 10^4 dilutions), and 3 μl of each cell suspension was spotted on YPD medium containing 0.75 M of NaCl or KCl and YPD medium containing 100 μg/ml fludioxonil or 2 mM or 2.5 mM of H_2O_2, 100 μg/ml fludioxonil. To test high-temperature and UV sensitivity, cells on YPD plates were incubated at 40°C and exposed to UV for 0.3 min (720 J/m^2). Cells were further incubated for 2 to 4 days and photographed.

fludioxonil sensitivity patterns of all 94 progeny (Fig. 2) (see Table S2 in the supplemental material), indicating that Ssk2 is likely the factor responsible for constitutive Hog1 phosphorylation in strain B-3501.

In *S. cerevisiae*, the molecular mechanism of Ssk2 MAPKKK interfacing between the Sln1-Ypd1-Ssk1 phosphorelay and the Pbs2-Hog1 pathways has been elegantly studied by Saito and others (26, 31, 33, 35). Under normal conditions, the Ssk1 response regulator is inactivated by phosphorylation transferred by Sln1 and Ypd1 (33). Furthermore, although the N-terminal RSD-I domain (*r*egulatory *s*ub*d*omain; amino acids 5 to 54) of Pbs2 constitutively binds to the kinase domain (KD) of Ssk2, the KD (amino acids 360 to 633) of Pbs2 itself is unable to gain access to the KD of Ssk2 due to an interaction between the N-terminal autoinhibitory domain (AID) and the C-terminal KD of Ssk2, which represses the Hog1 activation (35). In response to osmotic shock, Ssk1 becomes activated by dephosphorylation and subsequently binds to the AID of Ssk2, exposing the Ssk2 KD to the Pbs2 KD, which eventually phosphorylates and activates Hog1 (33). Supporting this model, elimination of the N-terminal AID of Ssk2 was found to result in constitutive phosphorylation and activation of Pbs2 and Hog1, which causes cell lethality (26).

The molecular mechanisms by which the *C. neoformans* two-component system consisting of Tco1/Tco2-Ypd1-Ssk1 is interconnected with the Ssk2-Pbs2-Hog1 MAPK module may not be directly deduced from that of *S. cerevisiae*, based on the following reasons. First, *C. neoformans* contains multiple hybrid HK systems (Tco1 to Tco7) and at least two (Tco1 and Tco2) positively regulate Hog1 (6). Second, constitutive phosphorylation of Hog1 does not appear to cause lethality, as corroborated by the finding that a majority of clinical *C. neoformans* strains contain a constitutively phosphorylated form of Hog1 (5). Nonetheless, the basic mechanism of Ssk2 regulation reported to occur in *S. cerevisiae*, relaying signals from Ssk1 to Pbs2, gives an important clue for understanding *C. neoformans* Ssk2 regulation. As can be seen from our findings, two nonsynonymous changes between strains B-3501 and JEC21 were located in the N-terminal region of Ssk2, different from the C-terminal KD domain. More interestingly, one of the two polymorphisms (L240F) resides in the putative Ssk1-binding domain of Ssk2 (Fig. 1C), implying that the N-terminal domain of Ssk2 may also play an important role in the precise regulation of the Pbs2-Hog1 pathway in *C. neoformans*.

Ssk2 MAPKKK is necessary and sufficient to control differential regulation of the Hog1 MAPK signaling pathway. To examine the role of Ssk2 in Hog1 MAPK signaling in *C. neoformans*, a mutational analysis was performed. The *SSK2* gene was disrupted by biolistic transformation and homologous recombination in both strain JEC21 (*ssk2-J*Δ) and strain B-3501 (*ssk2-B*Δ). In addition, the *PBS2* MAPKK gene was also disrupted in strain JEC21 (*pbs2-J*Δ). Similar to the *hog1*Δ mutant in the JEC21 background (*hog1-J*Δ), the *pbs2-J*Δ mutant exhibited hypersensitivity to osmotic shock and UV irradiation (Fig. 3). Interestingly, however, the *pbs2-J*Δ mutant did not show any unusual resistance to hydrogen peroxide (H_2O_2), a phenotype previously reported for the *hog1-J*Δ mutant (5), but did exhibit modest H_2O_2 hypersensitivity (Fig. 3). Previously, we have suggested that the unusual H_2O_2 resistance in the *hog1-J*Δ mutant is mediated independently of Hog1 MAPK kinase activity because a kinase-inactive *HOG1* allele completely restores the WT level of H_2O_2 sensitivity in the *hog1-J*Δ mutant (5).

Strain B-3501, in which Hog1 is constitutively phosphory-

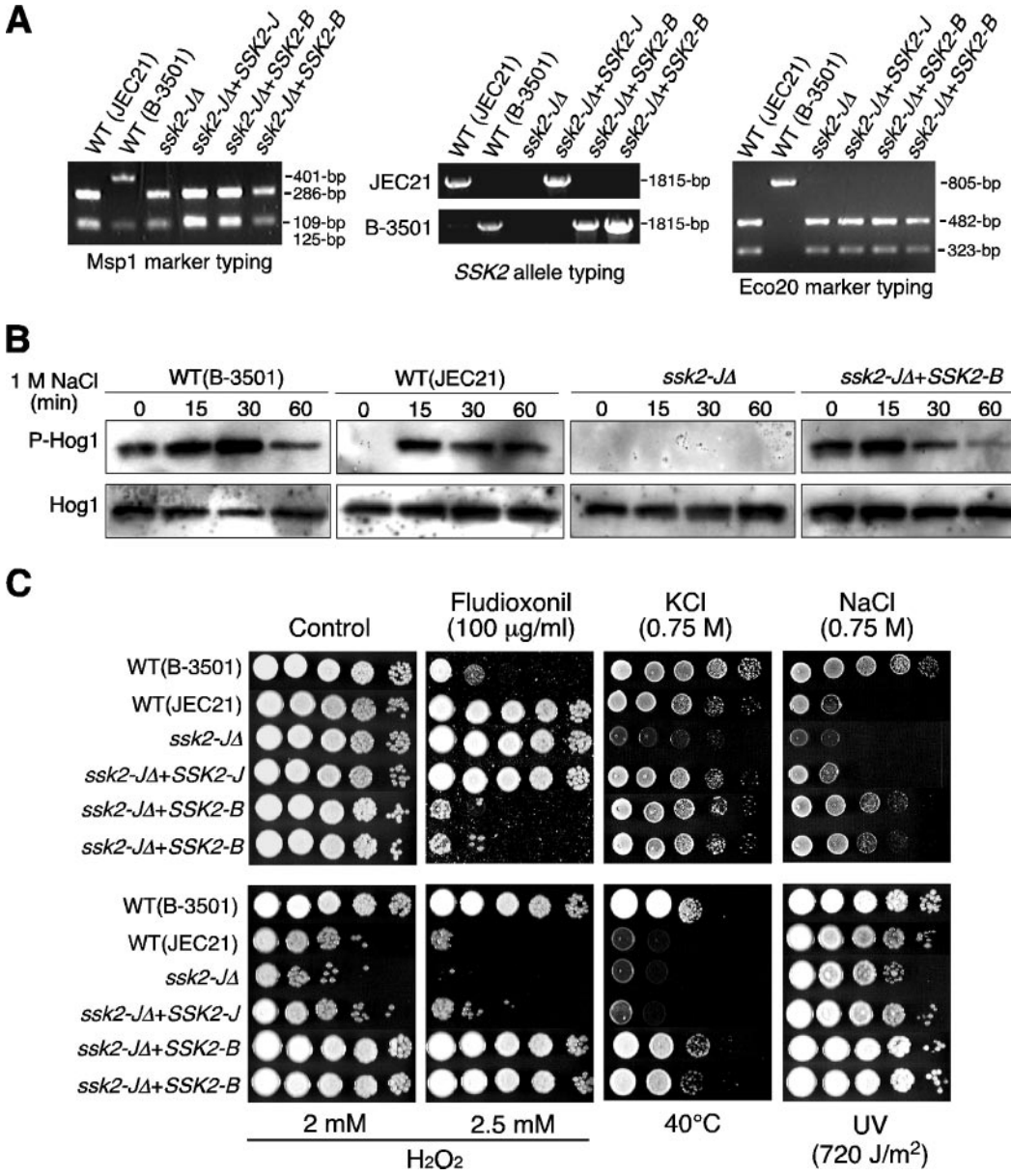

FIG. 4. Ssk2 MAPKKK is necessary and sufficient to govern differential stress responses. (A) Molecular genetic typing of *SSK2* allele-exchanged strains. The *SSK2* alleles and two genetic markers, MspI and Eco20, located upstream and downstream, respectively, of the *SSK2* allele, were PCR amplified by primers described in Table S1 in the supplemental material and analyzed by agarose gel electrophoresis. PCR products for MspI and Eco20 markers were digested with MspI and EcoRI and analyzed with a 1% agarose gel. (B) Each *C. neoformans* strain (WT JEC21, WT B-3501, YSB338 [*ssk2-J*Δ], and the *SSK2* allele-exchanged strain YSB392 [*ssk2-J*Δ+*SSK2-B*]) was grown to mid-logarithmic phase and exposed to 1 M NaCl in YPD medium for the time indicated, and total protein extracts were prepared for Western blot analysis. The dual phosphorylation status of Hog1 (T171 and Y173) was monitored using anti-dually phosphorylated p38 antibody (P-Hog1). The same blots were stripped and then reprobed with polyclonal anti-Hog1 antibody as a loading control (Hog1). (C) The stress sensitivity of each *C. neoformans* strain (WT JEC21, WT B-3501, YSB338 [*ssk2-J*Δ], the two *SSK2* allele-exchanged strains YSB392 and YSB394 [*ssk2-J*Δ+*SSK2-B*], and the *ssk2-J*Δ+*SSK2-J*-complemented strain YSB368) was monitored as described in the legend to Fig. 3. The same batch culture was used for both Fig. 3 and 4C.

lated similarly to the serotype A strain H99, generally showed higher stress resistance than strain JEC21 in terms of osmotic shock, UV irradiation, heat shock, and oxidative stress (Fig. 3). The *ssk2*Δ mutant in the JEC21 background (*ssk2-J*Δ) showed phenotypes comparable to those of the *pbs2-J*Δ mutant, which include hypersensitivity to osmotic shock, UV irradiation, and H_2O_2 (Fig. 3). Furthermore, the *ssk2*Δ mutant in the B-3501 background (*ssk2-B*Δ) exhibited hypersensitivity to osmotic shock, oxidative stress, high temperature, and UV irradiation (Fig. 3), phenotypes highly comparable to those of the *hog1*Δ and *pbs2*Δ mutants in serotype A (*hog1-A*Δ and *pbs2-A*Δ). Complementation of the *ssk2-J*Δ and *ssk2-B*Δ mutants with the WT *SSK2* allele restored the WT phenotypes (Fig. 3).

To verify that Ssk2 is a key signaling component responsible for the differential regulation of the Hog1 MAPK pathway, the *SSK2* alleles were exchanged between strains B-3501 and

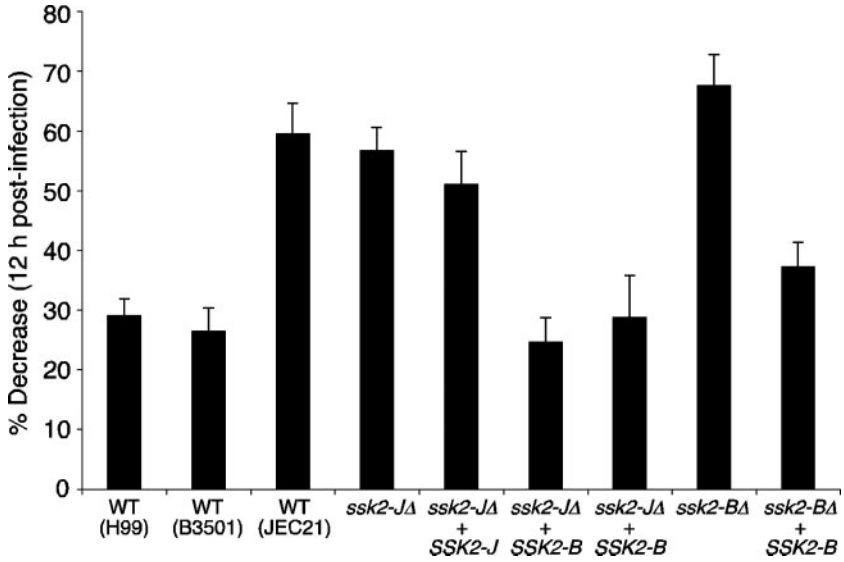

FIG. 5. The *SSK2* allele modulates sensitivity to the antifungal activities of murine macrophages. *C. neoformans* strains were incubated with MH-S cells at a multiplicity of infection of 1:1 for 12 h, and quantitative cultures were performed. Results are presented as percents decrease in CFU after 12 h compared to yeast-only control levels. The strains assessed are WT H99 [serotype A], WT B-3501 and JEC21 [serotype B], YSB338 [*ssk2-J*Δ], *ssk2-J*Δ+*SSK2-J*-complemented YSB368, *ssk2-J*Δ+*SSK2-B* allele-exchanged YSB392 and YSB394, YSB340 [*ssk2-B*Δ], and *ssk2-B*Δ+*SSK2-B*-complemented YSB391. Five replicates of each strain were examined in each experiment, and two independent experiments were performed. Significance was assessed using one-way analysis of variance (Bonferroni's multiple comparison test). A P value of <0.05 was considered significant. All strains containing the *SSK2-J* allele were significantly different from those containing the *SSK2-B* allele and vice versa ($P < 0.001$ for JEC21 versus B-3501; $P < 0.001$ for JEC21 versus YSB392 and YSB394 [*ssk2-J*Δ+*SSK2-B*]).

JEC21. For this purpose, the *ssk2-J*Δ mutant was biolistically transformed with a plasmid containing the B-3501 *SSK2* allele (*ssk2-J*Δ+*SSK2-B*). To confirm whether the B-3501 *SSK2* allele was specifically integrated into the JEC21 *SSK2* allele locus, the *SSK2* alleles and upstream and downstream genetic markers MspI and Eco20 were typed. The B-3501 *SSK2* allele was specifically integrated in the native *SSK2* locus of the *ssk2-J*Δ (YSB338) mutant in the two independent *SSK2* allele-exchanged strains (Fig. 4A). This *SSK2* allele exchange rendered JEC21 Hog1 constitutively phosphorylated under normal conditions, comparable to Hog1 in the B-3501 strain background (Fig. 4B). These data strongly indicate that Ssk2 mediates the difference in Hog1 phosphorylation between strains B-3501 and JEC21.

Two independent *SSK2* allele-exchanged strains (strain JEC21 with the B-3501 *SSK2* allele) were almost phenotypically identical to strain B-3501 (Fig. 4C). Although the JEC21 and *ssk2-J*Δ strains were resistant to fludioxonil, the two allele-exchanged strains (*ssk2-J*Δ+*SSK2-B*) were as sensitive to fludioxonil as strain B-3501 (Fig. 4C). In the case of osmotic-stress response (1 M NaCl), the *SSK2* allele exchange did not completely render strain JEC21 indistinguishable from strain B-3501. The *SSK2* allele-exchanged strains were less resistant to 1 M NaCl than strain B-3501 but were more resistant than strain JEC21 (Fig. 4C), possibly due to the polygenic nature of osmotic-stress response to 1 M NaCl. However, the allele-exchanged strains became as resistant to high temperature and oxidative stress as strain B-3501 (Fig. 4C), indicating that replacement of the *SSK2* allele renders strain JEC21 similar to strain B-3501 in terms of most stress responses and drug sensitivity. Notably, resistance to oxidative stress, osmotic stress, and high temperature appear to segregate as quantitative traits in the progeny of B-3501 crossed with B-3502, yet *SSK2* appears to play a central role in governing all of these phenotypic traits. This suggests that other genomic differences between strains B-3501 and JEC21 that are segregating in the cross but are not present in the JEC21 background may contribute or that other factors (such as epigenetic differences in meiotic progeny) may also play a role. Taken together, these data indicate that Ssk2 is a key upstream MAPKKK of the Pbs2-Hog1 MAPK pathway and is necessary and sufficient for differential regulation of the Hog1 MAPK in serotype D JEC21 and B-3501 strains.

The *SSK2* allele modulates sensitivity to the antifungal activities of murine macrophages. To further provide in vivo evidence supporting that Ssk2 is the key determinant for the virulence difference between JEC21 and B-3501, we performed a macrophage-killing assay with strains JEC21 and B3501 harboring divergent alleles of *SSK2*. The murine alveolar macrophage cell line (MH-S) was activated with gamma interferon and LPS prior to addition of *C. neoformans* strains. Mutant viability in response to macrophages was assessed by quantitative cultures and CFU counts. First, we found that strain B-3501 was as resistant to macrophage killing as strain H99 but exhibited greater levels of resistance than strain JEC21 (Fig. 5). Disruption of the *SSK2* gene did not significantly decrease the viability of strain JEC21, which is in agreement with the in vitro data showing a minor difference in oxidative-stress response between the JEC21 and *ssk2-J*Δ strains. In contrast, the *ssk2*Δ mutant in the B-3501 strain background (*ssk2-B*Δ) showed significantly reduced viability in the presence of macrophages compared to strain B-3501 (Fig. 5). Most notably, introduction of the B-3501 *SSK2* allele, but not the JEC21 *SSK2* allele, into the *ssk2-J*Δ mutant (*ssk2-J*Δ+*SSK2-B* strains)

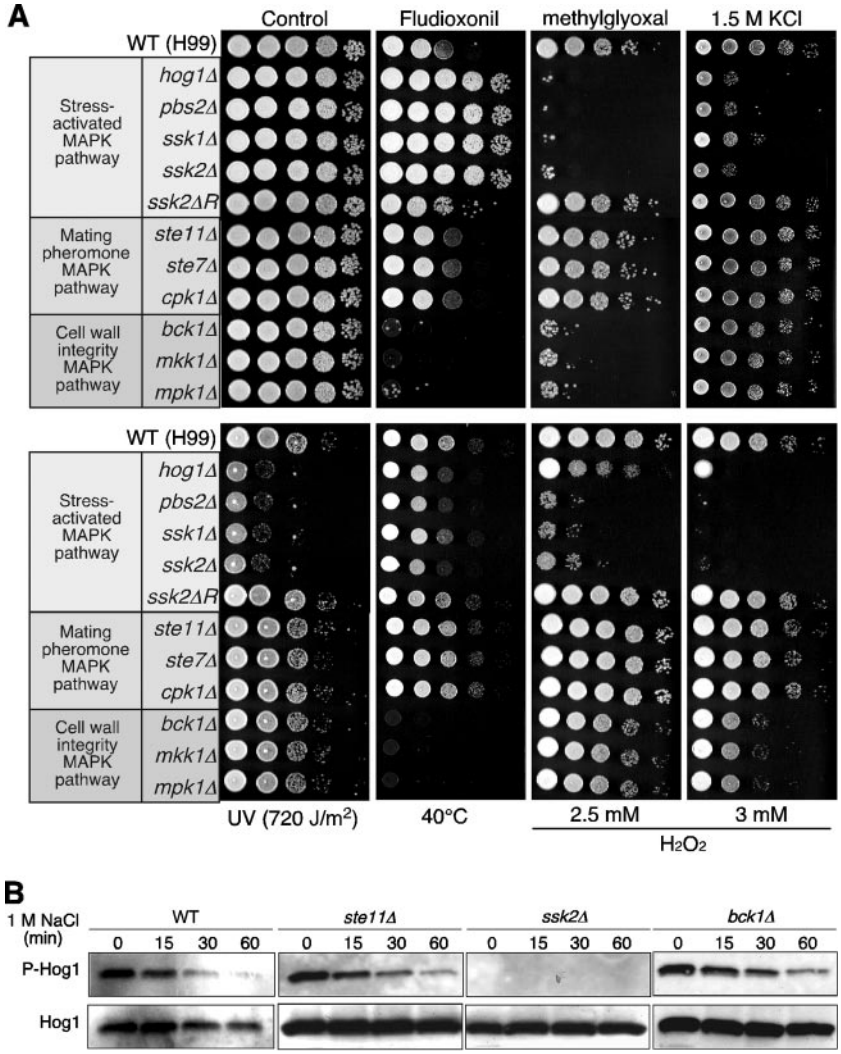

FIG. 6. Ssk2 is the only MAPKKK controlling the Pbs2-Hog1 pathway in the serotype A *C. neoformans* strain H99. (A) Each *C. neoformans* strain (WT H99 [serotype A], YSB64 [*hog1*Δ], YSB123 [*pbs2*Δ], YSB261 [*ssk1*Δ], YSB264 [*ssk2*Δ], YSB367 [*ssk2*Δ*R*; *ssk2*Δ+*SSK2* complemented], YSB313 [*ste11*Δ], YSB342 [*ste7*Δ], YSB127 [*cpk1*Δ], YSB273 [*bck1*Δ], YSB330 [*mkk1*Δ], and KK3 [*mpk1*Δ]) was grown to mid-logarithmic phase in YPD medium and 10-fold serially diluted (1 to 10^4 dilutions), and 3 μl of each cell suspension was spotted on YPD medium containing 1.5 M of KCl and YPD medium containing 100 μg/ml fludioxonil, 20 mM methylglyoxal, or 2.5 mM or 3 mM H_2O_2. To test high-temperature and UV sensitivity, cells on YPD plates were incubated at 40°C or exposed to UV for 0.3 min (720 J/m^2). Cells were further incubated for 2 to 4 days and photographed. (B) The *C. neoformans* serotype A WT strain (H99) and the *ste11*Δ (YSB313), *ssk2*Δ (YSB264), and *bck1*Δ (YSB273) mutant strains were grown to mid-logarithmic phase and exposed to 1 M NaCl in YPD medium for the time indicated, total protein extracts were prepared, and Western blot analysis was conducted as described for Fig. 4C.

significantly increased viability in the presence of macrophages (Fig. 5). These data indicate that Ssk2 plays a pivotal role in determining virulence differences between *C. neoformans* strains.

Ssk2 MAPKKK also governs the Pbs2-Hog1 MAPK pathway in serotype A. Identification of Ssk2 MAPKKK in the serotype D strains B-3501 and JEC21 led us to investigate the role of the Ssk2 MAPKKK homolog in the serotype A H99 strain, where the two-component system and the Pbs2-Hog1 pathway were previously investigated (6). Our prior study demonstrated that a two-component system composed of Tco1/Tco2-Ypd1-Ssk1 is a main upstream controller of the Pbs2-Hog1 signaling cascade (6). Upon osmotic shock (1 M NaCl), however, the Hog1 MAPK in the *ssk1*Δ mutant background was found to be phosphorylated although its constitutive phosphorylation levels were markedly reduced (6). These data indicate that *C. neoformans* Hog1, at least in the osmotic response, can be activated by multiple upstream branches (the Ssk1 response regulator and others) and Ssk2 MAPKKK may not be enough to fully control the Hog1 MAPK, similar to what occurs in *S. cerevisiae*, which expresses three MAPKKKs (Ssk2, Ssk22, and Ste11) that regulate Hog1.

By use of Ssk2 sequence information from the JEC21 and B-3501 genome databases, the serotype A Ssk2 homolog was identified through a tblastn search of the H99 genome database. To further address the role of Ssk2 in serotype A, the *SSK2* allele in the *MAT*α H99 and *MAT***a** KN99 strains was disrupted (*ssk2-A*Δ). As previously reported, the *hog1-A*Δ,

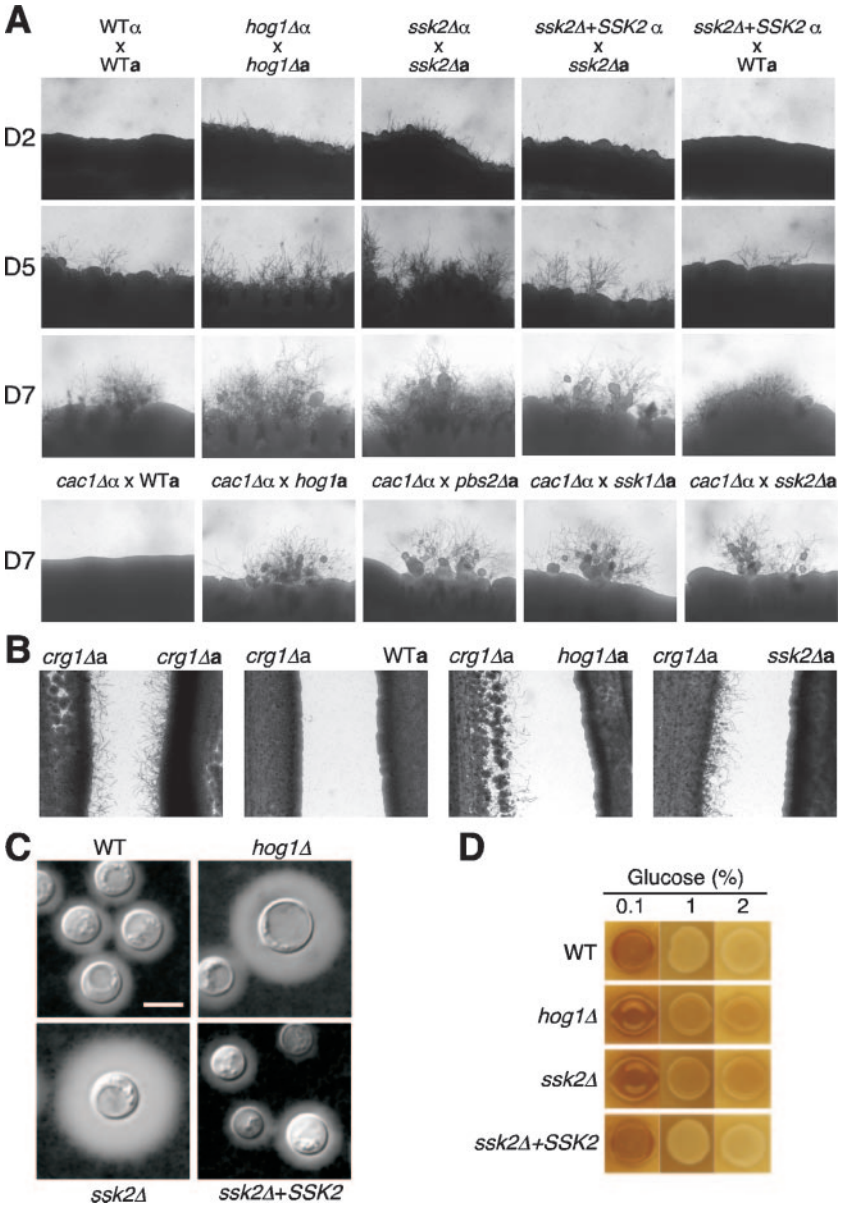

FIG. 7. *ssk2* mutation showed enhanced capsule and melanin production and sexual reproduction. (A) The following α and **a** strains were cocultured on V8 medium (pH 5.0) at room temperature in the dark: H99 with KN99**a** (WTα × WT**a**), YSB64 with YSB81 (*hog1*Δα × *hog1*Δ**a**), YSB264 with YSB441 (*ssk2*Δα × *ssk2*Δ**a**), YSB367 with YSB441 (*ssk2*Δ+*SSK2*α × *ssk2*Δ**a**), and YSB367 with KN99**a** (*ssk2*Δ+*SSK2*α × WT**a**). Representative edges of mating patches were photographed at ×100 magnification after 5 days of incubation. (B) The *crg1*Δ (H99 *crg1*) strain was confronted with the **a** *crg1*Δ (PPW196), KN99**a** (WT), YSB81 (*hog1*Δ), or YSB441 (*ssk2*Δ) strain, incubated for 7 days at room temperature in the dark, and photographed at ×40 magnification. (C) For capsule production, the H99 [WT], YSB64 [*hog1*Δ], YSB264 [*ssk2*Δ], and *ssk2*Δ+*SSK2*-complemented YSB367 strains were grown overnight (~16 h) in YPD medium, spotted on solid DMEM, incubated at 37°C for 2 days, and visualized by India ink staining. Bar, 10 μm. (D) For melanin production, the same strains were spotted on Niger seed medium containing 0.1%, 1%, or 2% glucose, incubated at 37°C for 3 days, and photographed.

*pbs2-A*Δ, and *ssk1-A*Δ mutants are hypersensitive to a variety of stresses, including osmotic shock, UV irradiation, high temperature, oxidative stress, and toxic metabolite, such as methylglyoxal, but completely resistant to the antifungal drug fludioxonil (Fig. 6A) (5, 6). Comparable to these mutants, *ssk2-A*Δ mutants exhibited similar stress responses and drug sensitivity (Fig. 6A).

In *S. cerevisiae*, the Pbs2-Hog1 MAPK pathway is controlled by three MAPKKKs, including Ssk2, Ssk22, and Ste11 (18). To address whether Ssk2 is the only MAPK controlling the Pbs2-Hog1 MAPK pathway in *C. neoformans*, we investigated other MAPKKKs. Based on the genome database, *C. neoformans* appears to have three major MAPKKKs: Ste11, Ssk2, and Bck1. To perform comparative phenotypic analysis of these MAPKKK mutants, we constructed *ste11*Δ, *ste7*Δ, and *cpk1*Δ mutants in the H99 strain by using the Nat^r dominant selectable marker. Mutants involved in cell wall integrity, including the *bck1*Δ, *mkk1*Δ, and *mpk1*Δ mutants, have been previously

constructed (22). Neither Ste11 nor Bck1 appears to control the Pbs2-Hog1 MAPK pathway. Cells harboring mutations in the mating-pheromone pathway consisting of Ste11 MAPKKK, Ste7 MAPKK, and Cpk1 MAPK were not more sensitive to stress or drug sensitive/resistant (Fig. 6A). In contrast to the *ssk2*Δ mutant, the *ste11*Δ and *bck1*Δ mutants were as resistant to osmotic shock and UV irradiation as WT H99 strains (Fig. 6A). Similarly, the Bck1-Mkk1-Mpk1 MAPK pathway controlling cell wall integrity is clearly distinct from the Ssk2-Pbs2-Hog1 MAPK pathway. First, the *bck1*, *mkk1*, and *mpk1* mutations did not change sensitivity to osmotic shock or UV irradiation (Fig. 6A). Second, the *bck1*Δ, *mkk1*Δ, and *mpk1*Δ mutants showed hypersensitivity to fludioxonil, to which the *ssk2*Δ, *pbs2*Δ, and *hog1*Δ mutants were completely resistant (Fig. 6A).

To further verify that Ssk2 is the only MAPKKK controlling the Pbs2-Hog1 MAPK pathway, Hog1 MAPK phosphorylation patterns were monitored in response to osmotic shock (1 M NaCl) (Fig. 6B). In the cases of the *ste11*Δ and *bck1*Δ mutants, which are as resistant to osmotic shock as the WT, Hog1 became dephosphorylated in response to 1 M NaCl (Fig. 6B). As expected, however, Hog1 phosphorylation was completely absent in the *ssk2*Δ mutant (Fig. 6B). These data indicate that Ssk2 is necessary and sufficient to control the Pbs2-Hog1 MAPK pathway.

Recently, Cheetham et al. reported that *C. albicans* also employs a single MAPKKK (Ssk2) to control the Hog1 MAPK (10). In *C. albicans*, the homozygous *ssk2*/*ssk2* mutant exhibits stress responses and morphological phenotypes (hyperfilamentation) comparable to those observed in the *hog1*/*hog1* mutant whereas the *ste11*/*ste11* mutant does not show any Hog1-related phenotypes (10). Supporting this finding, Román et al. previously demonstrated that *C. albicans* Sho1, which is homologous to the *S. cerevisiae* Sho1 osmosensor that functions upstream of the Ste11 MAPKKK, does not relay osmotic-stress signals to Hog1 (34). Similarly, Sho1 is also dispensable for osmoregulation in *Aspergillus nidulans* (13). In contrast, however, both the Sho1-Ste11 and the Ssk2 MAPKKK signaling branches control Hog1-dependent osmoregulation in *Candida glabrata* (15). In *C. neoformans*, no Sho1 homologue was apparent in the completed genome (7).

Ssk2 MAPKKK controls morphological differentiation and virulence factor production. Previously, the Pbs2-Hog1 MAPK pathway was shown to negatively control morphological differentiation as well as two major virulence factors, capsule and melanin (5). To further corroborate whether Ssk2 MAPKKK governs the Pbs2-Hog1 MAPK pathway, the mating ability of the *ssk2*Δ mutant was compared with those of the WT strains and *hog1*Δ mutants. Similar to the *hog1*Δ mutants, the *ssk2*Δ mutants showed higher mating capabilities than the WT strains (Fig. 7A). Furthermore, in mating with a defective mating partner, the *cac1*Δ mutant (*MAT*α), the *MAT***a** *ssk2*Δ mutant showed increased mating efficiency, similar to the *MAT***a** *hog1*Δ, *pbs2*Δ, and *ssk1*Δ mutants (Fig. 7A). In a previous report, *hog1*Δ mutants exhibit enhanced mating due to derepressed pheromone production (5). In confrontation assays using the pheromone-hypersensitive *crg1*Δ mutants, which lack an RGS protein that normally desensitizes the pheromone response pathway (29, 36), *ssk2*Δ mutants were as effective in inducing pheromone-mediated conjugation tubes as *crg1*Δ and *hog1*Δ mutants (Fig. 7B). These results indicate that Ssk2 also negatively regulates the mating-pheromone MAPK pathway by controlling the Pbs2-Hog1 MAPK pathway.

Two major *C. neoformans* virulence factors, capsule and melanin, are controlled by the cAMP signaling pathway (2–4, 17). Mutations in any signaling components in the pathway drastically reduce capsule and melanin production and result in decreased virulence. Previously, we have found that capsule and melanin biosyntheses are negatively regulated by the Pbs2-Hog1 MAPK pathway, potentially via cross talk with the cAMP pathway (5). Here, the *ssk2*Δ mutant was also found to be enhanced in both capsule and melanin production, similar to the *hog1*Δ mutant (Fig. 7C and D). Taken together, these data indicate that Ssk2 is the key upstream MAPKKK controlling the Pbs2-Hog1 MAPK pathway.

In summary, Ssk2 is demonstrated to be a key signaling component determining differential phosphorylation patterns of Hog1 MAPK in diverse serotype A and D *C. neoformans* strains. Ssk2 plays a key role in interconnecting the Tco1/Tco2-Ypd1-Ssk1 two-component system with the Pbs2 MAPKK-Hog1 MAPK pathway to control stress responses to diverse environmental stimuli and drug sensitivity in *C. neoformans*. Furthermore, the serotype A *C. neoformans ssk2*Δ mutant, but not the *bck1*Δ or *ste11*Δ mutant, exhibits phenotypes identical to those of the *pbs2*Δ and *hog1*Δ mutants, indicating that Ssk2 is necessary and sufficient as the MAPKKK for the Pbs2-Hog1 MAPK pathway in *C. neoformans*. To our knowledge, this study not only characterized the role of Ssk2 MAPKKK in *C. neoformans* for the first time but also provides insights for understanding the evolution of virulence attributes of pathogens by demonstrating that changing a single signaling component can dramatically alter virulence characteristics.

The exact molecular mechanism leading to constitutive phosphorylation of Hog1 in the serotype A H99 strain remains to be elucidated at a molecular level. Compared to what occurs in the stress-sensitive JEC21 strain, two polymorphic residues, L248 and M738, observed in B-3501 and H99, might not be the only residues contributing to constitutive phosphorylation of Hog1, particularly in strain H99, because the phosphorylation level of Hog1 in strain H99 is even higher than that in strain B-3501 (5). Therefore, other structural features of serotype A Ssk2 may further contribute to constitutive phosphorylation of Hog1 MAPK. This possibility is currently under investigation.

ACKNOWLEDGMENTS

We thank Robert E. Marra, Thomas G. Mitchell, and Kirsten Nielsen for assistance with linkage analysis and Jo Rae Wright for help with macrophage-killing assays.

This work was supported by the Soongsil University Research Fund to Y.-S. Bahn, by NIH grant HL-30923 to S. Geunes-Boyer, and by NIH RO1 grant AI39115 and R21 grant AI070230 to J. Heitman.

REFERENCES

1. **Alonso-Monge, R., F. Navarro-Garcia, G. Molero, R. Diez-Orejas, M. Gustin, J. Pla, M. Sanchez, and C. Nombela.** 1999. Role of the mitogen-activated protein kinase Hog1p in morphogenesis and virulence of *Candida albicans*. J. Bacteriol. **181:**3058–3068.
2. **Alspaugh, J. A., J. R. Perfect, and J. Heitman.** 1997. *Cryptococcus neoformans* mating and virulence are regulated by the G-protein alpha subunit GPA1 and cAMP. Genes Dev. **11:**3206–3217.
3. **Alspaugh, J. A., R. Pukkila-Worley, T. Harashima, L. M. Cavallo, D. Funnell, G. M. Cox, J. R. Perfect, J. W. Kronstad, and J. Heitman.** 2002. Adenylyl cyclase functions downstream of the Gα protein Gpa1 and controls mating and pathogenicity of *Cryptococcus neoformans*. Eukaryot. Cell **1:**75–84.

4. **Bahn, Y. S., J. K. Hicks, S. S. Giles, G. M. Cox, and J. Heitman.** 2004. Adenylyl cyclase-associated protein Aca1 regulates virulence and differentiation of *Cryptococcus neoformans* via the cyclic AMP-protein kinase A cascade. Eukaryot. Cell **3:**1476–1491.
5. **Bahn, Y. S., K. Kojima, G. M. Cox, and J. Heitman.** 2005. Specialization of the HOG pathway and its impact on differentiation and virulence of *Cryptococcus neoformans*. Mol. Biol. Cell **16:**2285–2300.
6. **Bahn, Y. S., K. Kojima, G. M. Cox, and J. Heitman.** 2006. A unique fungal two-component system regulates stress responses, drug sensitivity, sexual development, and virulence of *Cryptococcus neoformans*. Mol. Biol. Cell **17:**3122–3135.
7. **Bahn, Y. S., C. Xue, A. Idnurm, J. C. Rutherford, J. Heitman, and M. E. Cardenas.** 2007. Sensing the environment: lessons from fungi. Nat. Rev. Microbiol. **5:**57–69.
8. **Brewster, J. L., T. de Valoir, N. D. Dwyer, E. Winter, and M. C. Gustin.** 1993. An osmosensing signal transduction pathway in yeast. Science **259:**1760–1763.
9. **Catlett, N. L., O. C. Yoder, and B. G. Turgeon.** 2003. Whole-genome analysis of two-component signal transduction genes in fungal pathogens. Eukaryot. Cell **2:**1151–1161.
10. **Cheetham, J., D. A. Smith, A. da Silva Dantas, K. S. Doris, M. J. Patterson, C. R. Bruce, and J. Quinn.** 2007. A single MAPKKK regulates the Hog1 MAPK pathway in the pathogenic fungus *Candida albicans.* Mol. Biol. Cell. **18:**4603–4614.
11. **Davidson, R. C., J. R. Blankenship, P. R. Kraus, M. de Jesus Berrios, C. M. Hull, C. D'Souza, P. Wang, and J. Heitman.** 2002. A PCR-based strategy to generate integrative targeting alleles with large regions of homology. Microbiology **148:**2607–2615.
12. **Davidson, R. C., M. C. Cruz, R. A. Sia, B. Allen, J. A. Alspaugh, and J. Heitman.** 2000. Gene disruption by biolistic transformation in serotype D strains of *Cryptococcus neoformans*. Fungal Genet. Biol. **29:**38–48.
13. **Furukawa, K., Y. Hoshi, T. Maeda, T. Nakajima, and K. Abe.** 2005. *Aspergillus nidulans* HOG pathway is activated only by two-component signalling pathway in response to osmotic stress. Mol. Microbiol. **56:**1246–1261.
14. **Granger, D. L., J. R. Perfect, and D. T. Durack.** 1985. Virulence of *Cryptococcus neoformans*. Regulation of capsule synthesis by carbon dioxide. J. Clin. Investig. **76:**508–516.
15. **Gregori, C., C. Schuller, A. Roetzer, T. Schwarzmuller, G. Ammerer, and K. Kuchler.** 2007. The high-osmolarity glycerol response pathway in the human fungal pathogen *Candida glabrata* Strain ATCC 2001 lacks a signaling branch that operates in baker's yeast. Eukaryot. Cell **6:**1635–1645.
16. **Heitman, J., B. Allen, J. A. Alspaugh, and K. J. Kwon-Chung.** 1999. On the origins of congenic *MAT*α and *MAT***a** strains of the pathogenic yeast *Cryptococcus neoformans*. Fungal Genet. Biol. **28:**1–5.
17. **Hicks, J. K., C. A. D'Souza, G. M. Cox, and J. Heitman.** 2004. Cyclic AMP-dependent protein kinase catalytic subunits have divergent roles in virulence factor production in two varieties of the fungal pathogen *Cryptococcus neoformans*. Eukaryot. Cell **3:**14–26.
18. **Hohmann, S.** 2002. Osmotic stress signaling and osmoadaptation in yeasts. Microbiol. Mol. Biol. Rev. **66:**300–372.
19. **Idnurm, A., Y. S. Bahn, K. Nielsen, X. Lin, J. A. Fraser, and J. Heitman.** 2005. Deciphering the model pathogenic fungus *Cryptococcus neoformans*. Nat. Rev. Microbiol. **3:**753–764.
20. **Johnson, G. L., and R. Lapadat.** 2002. Mitogen-activated protein kinase pathways mediated by ERK, JNK, and p38 protein kinases. Science **298:**1911–1912.
21. **Kawasaki, L., O. Sanchez, K. Shiozaki, and J. Aguirre.** 2002. SakA MAP kinase is involved in stress signal transduction, sexual development and spore viability in *Aspergillus nidulans*. Mol. Microbiol. **45:**1153–1163.
22. **Kojima, K., Y. S. Bahn, and J. Heitman.** 2006. Calcineurin, Mpk1 and Hog1 MAPK pathways independently control fludioxonil antifungal sensitivity in *Cryptococcus neoformans*. Microbiology **152:**591–604.
23. **Kojima, K., Y. Takano, A. Yoshimi, C. Tanaka, T. Kikuchi, and T. Okuno.** 2004. Fungicide activity through activation of a fungal signalling pathway. Mol. Microbiol. **53:**1785–1796.
24. **Kwon-Chung, K. J., J. C. Edman, and B. L. Wickes.** 1992. Genetic association of mating types and virulence in *Cryptococcus neoformans*. Infect. Immun. **60:**602–605.
25. **Lee, J. C., S. Kumar, D. E. Griswold, D. C. Underwood, B. J. Votta, and J. L. Adams.** 2000. Inhibition of p38 MAP kinase as a therapeutic strategy. Immunopharmacology **47:**185–201.
26. **Maeda, T., M. Takekawa, and H. Saito.** 1995. Activation of yeast PBS2 MAPKK by MAPKKKs or by binding of an SH3-containing osmosensor. Science **269:**554–558.
27. **Marra, R. E., J. C. Huang, E. Fung, K. Nielsen, J. Heitman, R. Vilgalys, and T. G. Mitchell.** 2004. A genetic linkage map of *Cryptococcus neoformans* variety *neoformans* serotype D (*Filobasidiella neoformans*). Genetics **167:**619–631.
28. **Millar, J. B., V. Buck, and M. G. Wilkinson.** 1995. Pyp1 and Pyp2 PTPases dephosphorylate an osmosensing MAP kinase controlling cell size at division in fission yeast. Genes Dev. **9:**2117–2130.
29. **Nielsen, K., G. M. Cox, P. Wang, D. L. Toffaletti, J. R. Perfect, and J. Heitman.** 2003. Sexual cycle of *Cryptococcus neoformans* var. *grubii* and virulence of congenic **a** and α isolates. Infect. Immun. **71:**4831–4841.
30. **Perfect, J. R., N. Ketabchi, G. M. Cox, C. W. Ingram, and C. L. Beiser.** 1993. Karyotyping of *Cryptococcus neoformans* as an epidemiological tool. J. Clin. Microbiol. **31:**3305–3309.
31. **Posas, F., and H. Saito.** 1998. Activation of the yeast SSK2 MAP kinase kinase kinase by the SSK1 two-component response regulator. EMBO J. **17:**1385–1394.
32. **Posas, F., and H. Saito.** 1997. Osmotic activation of the HOG MAPK pathway via Ste11p MAPKKK: scaffold role of Pbs2p MAPKK. Science **276:**1702–1705.
33. **Posas, F., S. M. Wurgler-Murphy, T. Maeda, E. A. Witten, T. C. Thai, and H. Saito.** 1996. Yeast HOG1 MAP kinase cascade is regulated by a multistep phosphorelay mechanism in the SLN1-YPD1-SSK1 "two-component" osmosensor. Cell **86:**865–875.
34. **Román, E., C. Nombela, and J. Pla.** 2005. The Sho1 adaptor protein links oxidative stress to morphogenesis and cell wall biosynthesis in the fungal pathogen *Candida albicans*. Mol. Cell. Biol. **25:**10611–10627.
35. **Tatebayashi, K., M. Takekawa, and H. Saito.** 2003. A docking site determining specificity of Pbs2 MAPKK for Ssk2/Ssk22 MAPKKKs in the yeast HOG pathway. EMBO J. **22:**3624–3634.
36. **Wang, P., J. Cutler, J. King, and D. Palmer.** 2004. Mutation of the regulator of G protein signaling Crg1 increases virulence in *Cryptococcus neoformans*. Eukaryot. Cell **3:**1028–1035.